Electronic Supplementary Information

Fluorescent Zinc(II) Complexes for Gene Delivery and Simultaneous Monitoring of Protein Expression

*Lalita B. Rane[a], Anup N. Kate[a], Shefali N. Ramteke[b], Bhupendra V. Shravage[c], Prasad P. Kulkarni[b] and Anupa A. Kumbhar[a]**

[a]Department of Chemistry, SavitribaiPhulePuneUniversity, Pune – 411007, India

[b]Bioprospecting Group, Agharkar Research Institute, Pune-411004, India.

[c]Developmental Biology Group, Agharkar Research Institute, Pune-411004, India.

Scheme S1: Synthetic route for 1 and 2

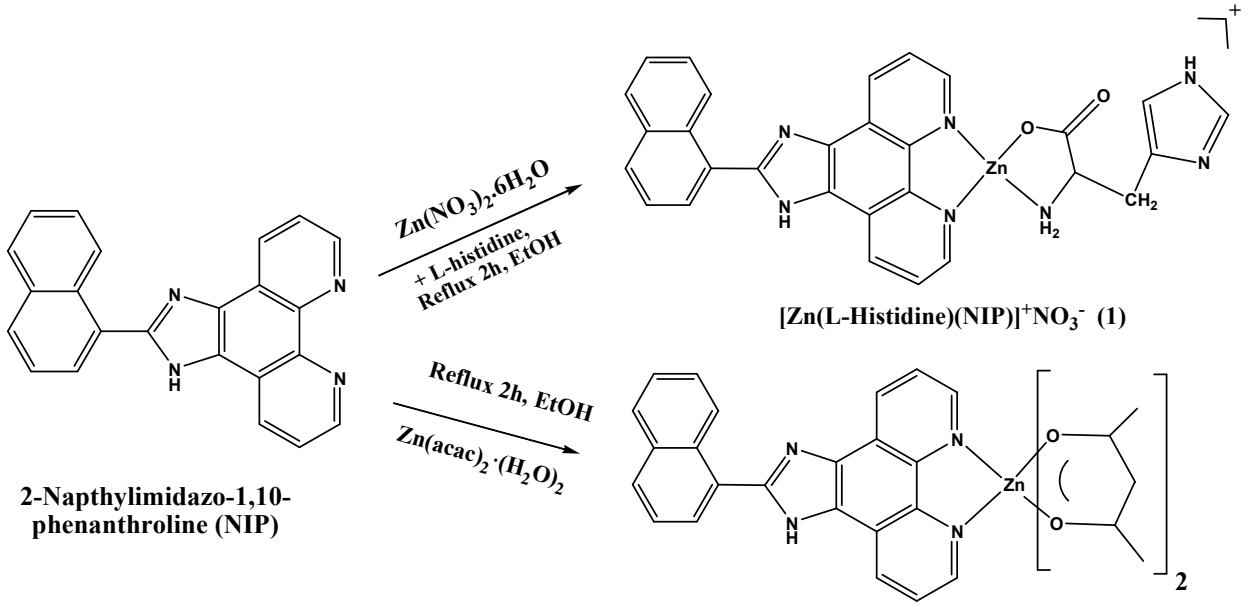

Table S1: List of intrinsic binding constants (K_b) of various transition metal complexescontaining IP and acac as one of the ligands

Complex	K_b (M^{-1})	References
$[Cu(nip)(acac)]^+$	7.5×10^4	1
$[Cu(NIP)_2]^{2+}$	9.69×10^4	1
$[Co\ (Phen)_2(PIP)]^{3+}$	2.15×10^5	2
$[Co(bpy)_2(PIP)]^{3+}$	1.9×10^5	2
$[Co(phen)_2(ippip)]^{3+}$	$1.9\pm0.2\times10^5$	3
$[Co(bpy)_2(CNOIP)]^{3+}$	5.0×10^4	4
$[Co(Phen)_2(CNOIP)]^{3+}$	1.6×10^5	4
$[Co(Phen)_2(HPIP)]^{3+}$	4.1×10^5	5
$[Co(Phen)_2(HNAIP)]^{3+}$	1.8×10^5	5
$[Ru(bpy)_2(BPIP)]^{2+}$	1.70×10^5	6
$[Ru(Phen)_2(BPIP)]^{2+}$	7.03×10^4	6
$[Ru(bpy)_2(PPIP)]^{2+}$	4.3×10^4	7
$[Ru(Phen)_2(PPIP)]^{2+}$	1.1×10^5	7
$[Ru(bpy)_2(PIP)]^{2+}$	$4.7\pm0.2 \times10^5$	8
$[Ru(phen)_2(ippip)]^{2+}$	$2.1\pm0.2\times10^5$	3
[Cu(acac)(dpq)Cl]	2.2×10^5	9
[Cu(acac)(dppz)Cl]	3.6×10^5	9
$[Cu(biim)(acac)(H_2O)]_2[Cu(acac)_2(ClO_4)_2]$	3.6×10^5	10
$[Zn(L\text{-}His)(NIP)]^+$**(1)**	3.3×10^5	Present work
$[Zn(acac)_2(NIP)]$ (**2**)	1.76×10^4	Present work

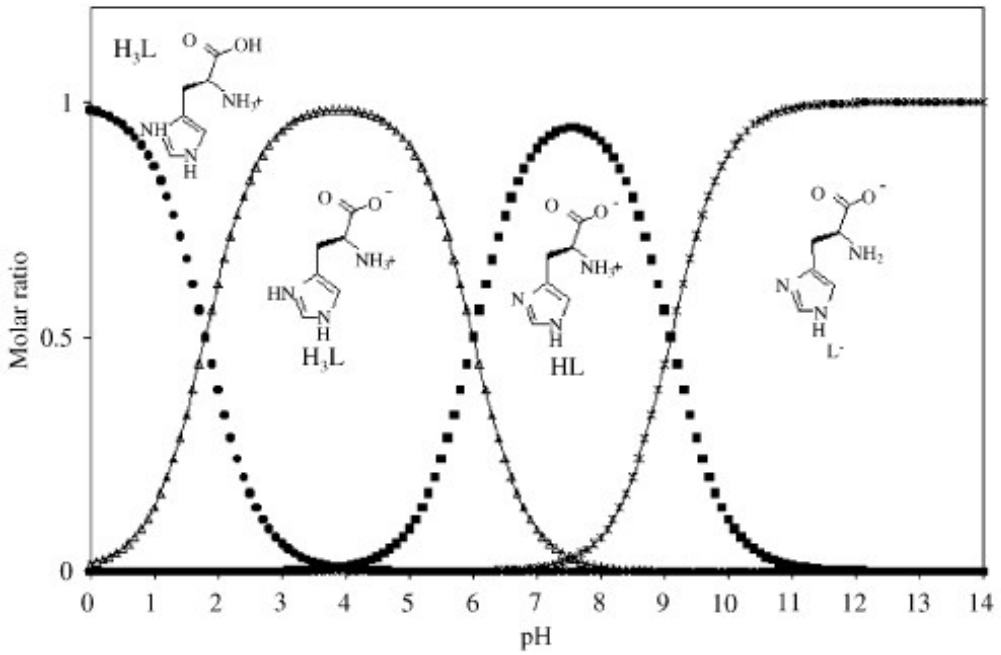

Fig. S1: Speciation diagram for L-histidine showing that the major form of L-histidine at pH ~ 11 is L^- (Adapted from P. Deschamps, P.P. Kulkarni, M. Gautam-Basak, and B. Sarkar *Coord. Chem. Rev*. 2005, **249**, 895–909)

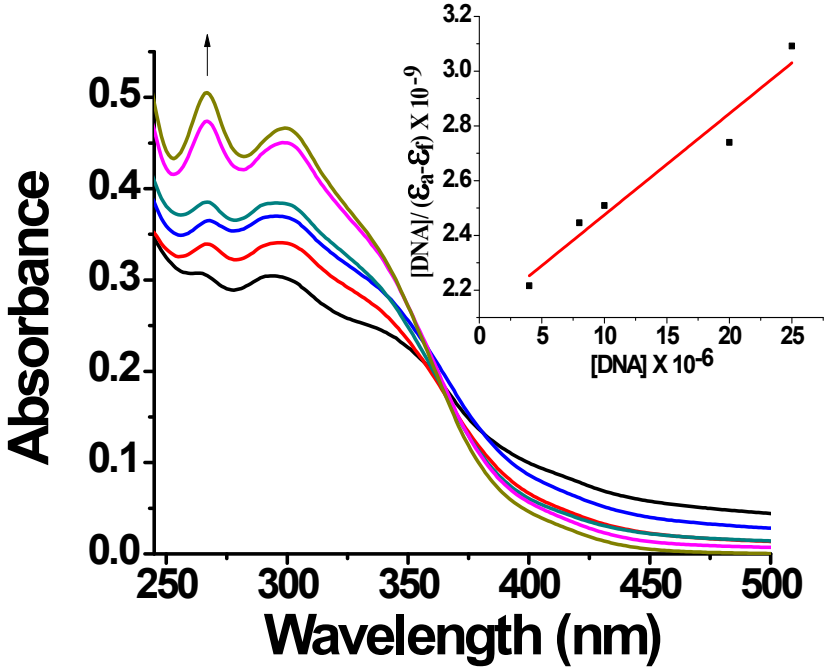

Fig. S2: Electronic absorption spectra of **2** in absence and presence of increasing amounts of CT-DNA. Inset: Plot of [DNA]/(ε_a-ε_f) vs. [DNA].

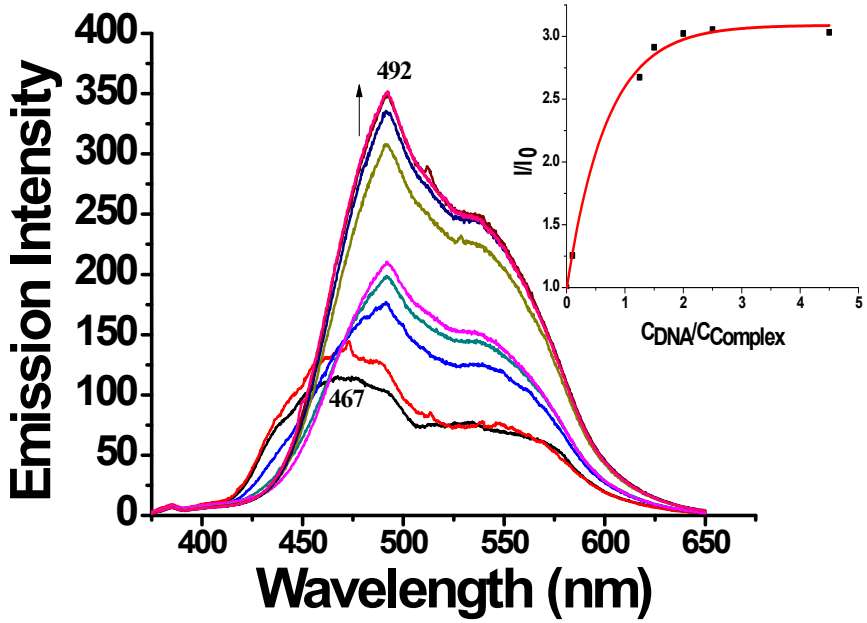

Fig. S3: Emission spectra (λ_{ex} = 341 nm) of **2** in absence and presence of CT-DNA, [**2**] = 20 μM.

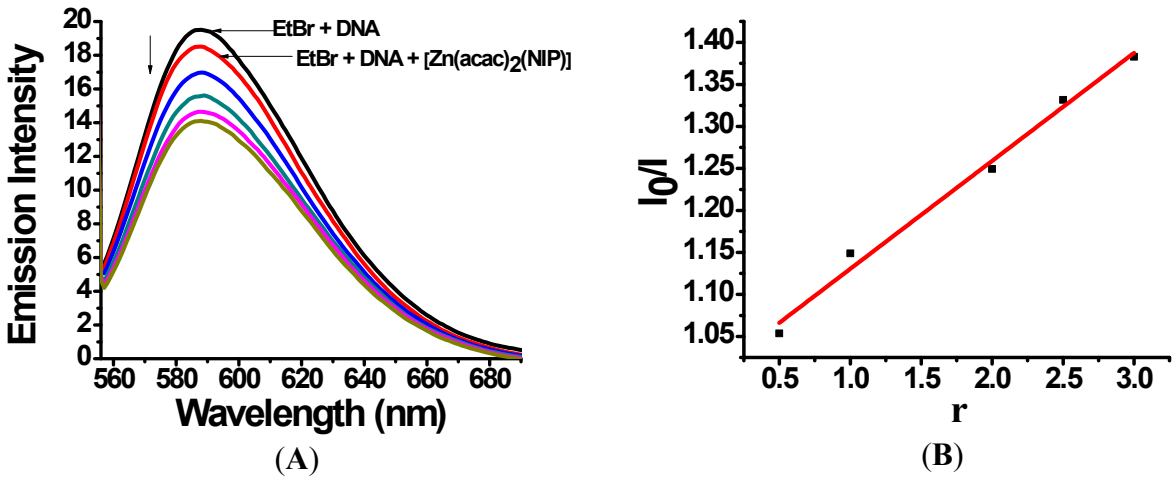

Fig. S4: (**A**) The fluorescence spectra of the binding of EtBr to CT-DNA in phosphate buffer at pH 7.2, in the absence and presence of increasing amounts of **2**, [**2**] = 0 – 30 µM, [DNA] = 10 µM. (**B**) Stern-Volmer quenching plot of CT-DNA – EtBr system by [**2**], r = $C_{complex}$/ C_{DNA}.

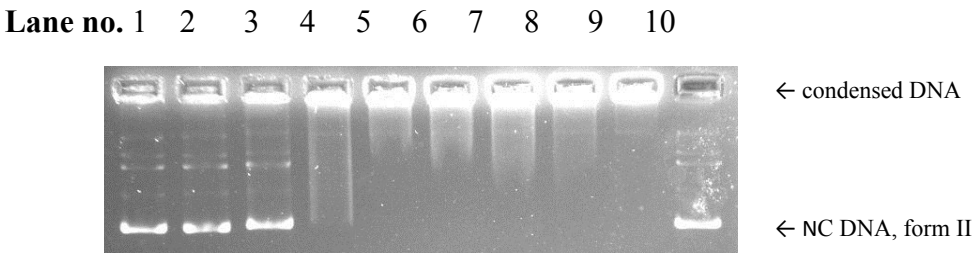

Fig. S5: Agarose gel electrophoresis of pBR322 DNA, [**2**] = 10–500µM, [DNA] = 100ng/µL, incubation time = 30 min., TBE buffer, pH 7.2, 37°C. Lanes 1: DNA control, Lane 10: DNA control + DMSO, Lane 2-9: DNA + [**2**](10, 20, 50, 100, 200, 300, 400, 500 µM respectively).

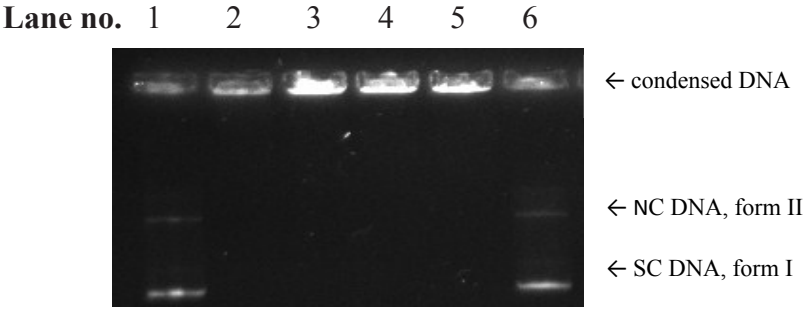

Fig.S6: Effect of high concentration of NaCl on reversibility of pBR322 DNA condensation induced by **1** in phosphate buffer (pH 7.2) Lane 1: control, nonmodified DNA, Lane 2: DNA + complex (1.2 mM), Lane 3: DNA + **1** (1.2 mM) + NaCl (0.25 M), Lane 4:DNA + **1** (1.2 mM) + NaCl (0.45 M), Lane 5: DNA + **1** (1.2 mM) + NaCl (0.65 M), Lane 6: DNA + DMSO.

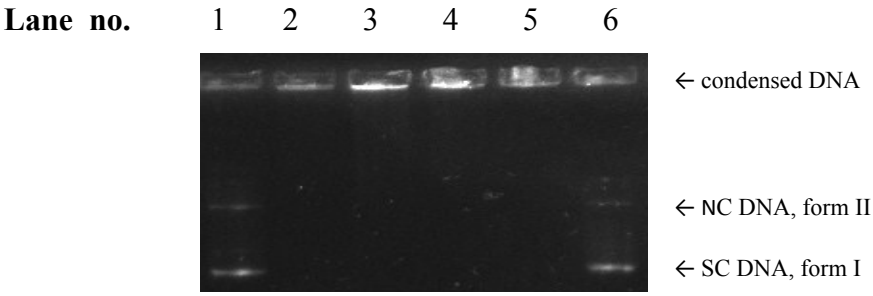

Fig.S7: Effect of high concentration of NaCl on reversibility of pBR322 DNA condensation induced by **2** in phosphate buffer (pH 7.2) Lane 1: control, nonmodified DNA, Lane 2: DNA + **2** (1.2 mM), Lane 3: DNA + **2**(1.2 mM) + NaCl (0.25 M), Lane 4:DNA + **2** (1.2 mM) + NaCl (0.45 M), Lane 5: DNA + **2**(1.2 mM) + NaCl (0.65 M), Lane 6: DNA + DMSO.

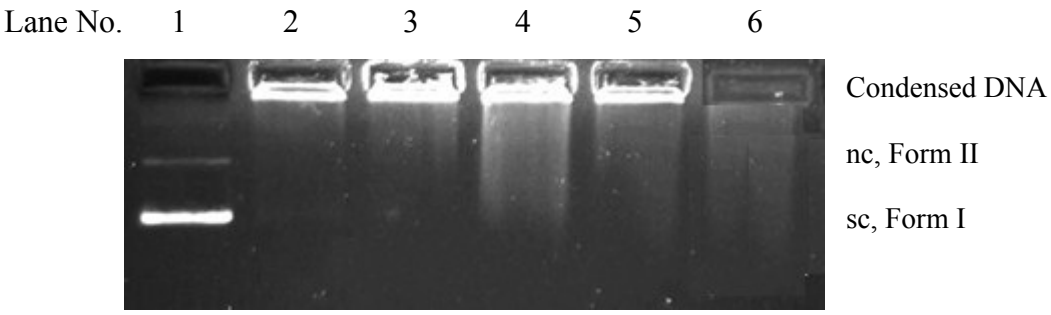

Fig. S8: Agarose gel electrophoresis pattern of pBR322 DNA, showing the protection of plasmid pBR322 DNA against DNase I (10 units) by preformed DNA condensates of **1** and **2**. [DNA] =100 ng, [**1** and **2**] = 200 μM. Lane 1: DNA control, Lane 2: DNA + **1** (200 μM); Lane 3: DNA + **1** (200 μM) +DNase I; Lane 4: DNA + **2** (200 μM); Lane 5: DNA + **2** (200 μM) + DNase I; Lane 6: DNA + DNase I.

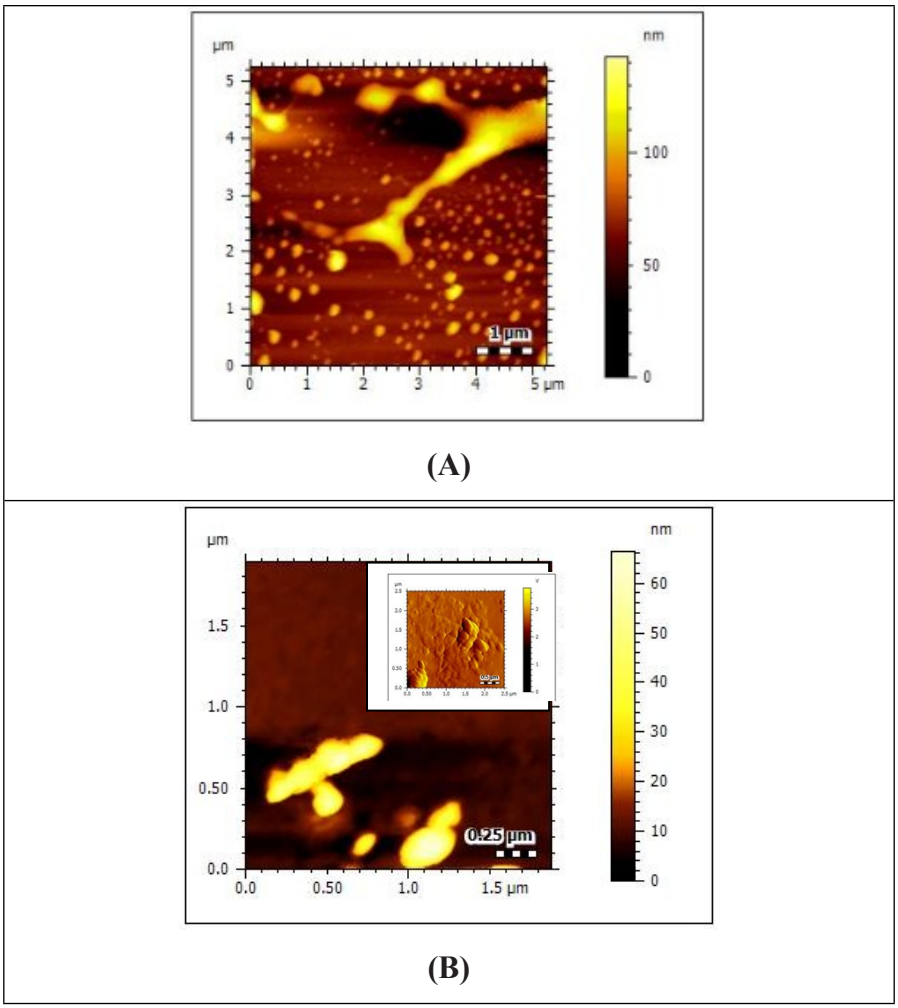

Fig. S9: AFM images of DNA condensates showing formation of bigger aggregates (conglomerates) on incubation of DNA (200 ng/µL) with 150 µM **(A) 1** (scan are 1 µm) and **(B) 2** (scan area 0.25 µm) in phosphate buffer (pH 7.2) for 60 min at 37ºC.

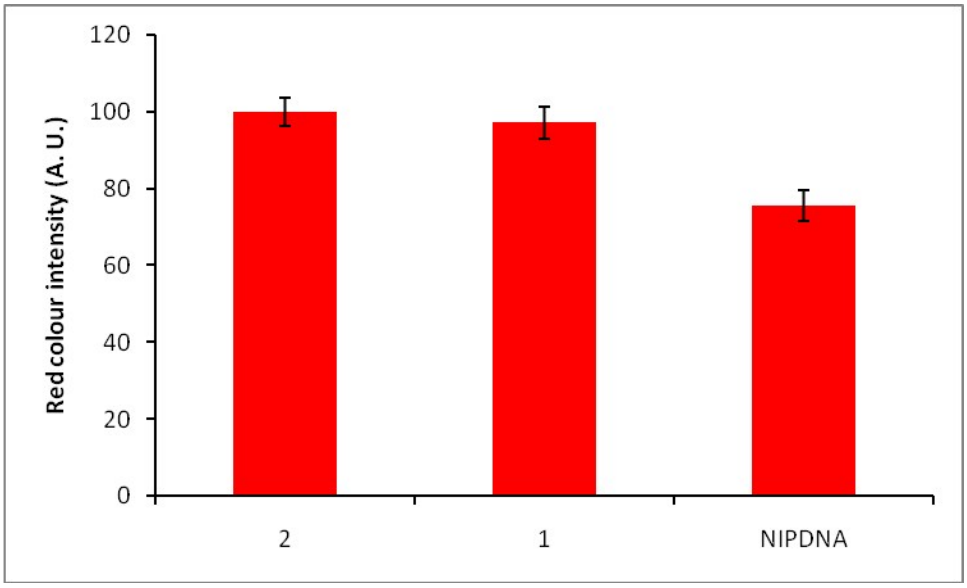

Fig. S10. The relative transfection efficiency of NIP alone and Zn(II) complexes (**1** and 2) calculated using Image J analysis.

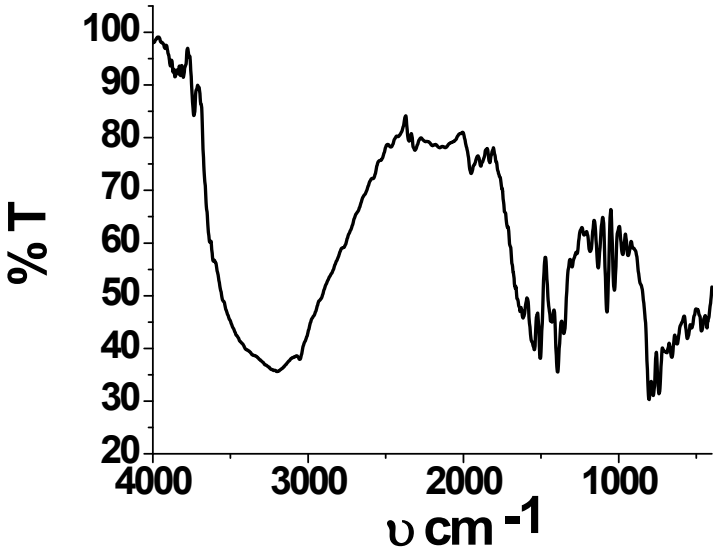

Fig. S11:IR spectrum of the ligand **NIP**.

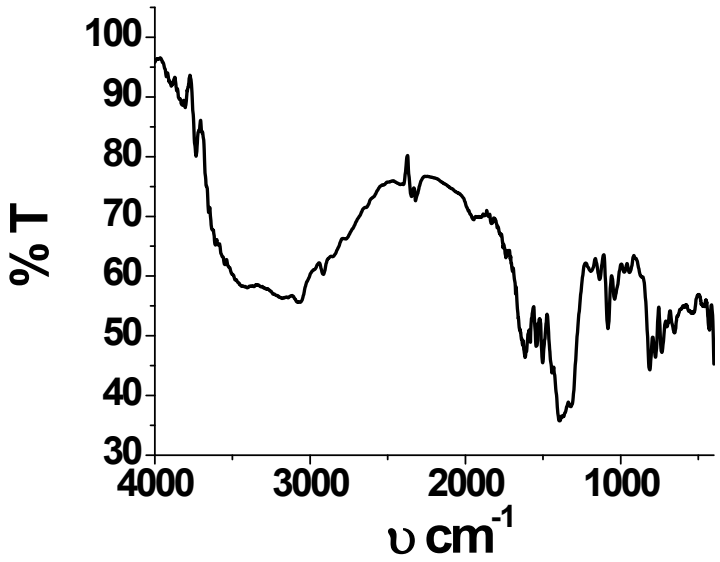

Fig. S12: IR spectrum of **1**.

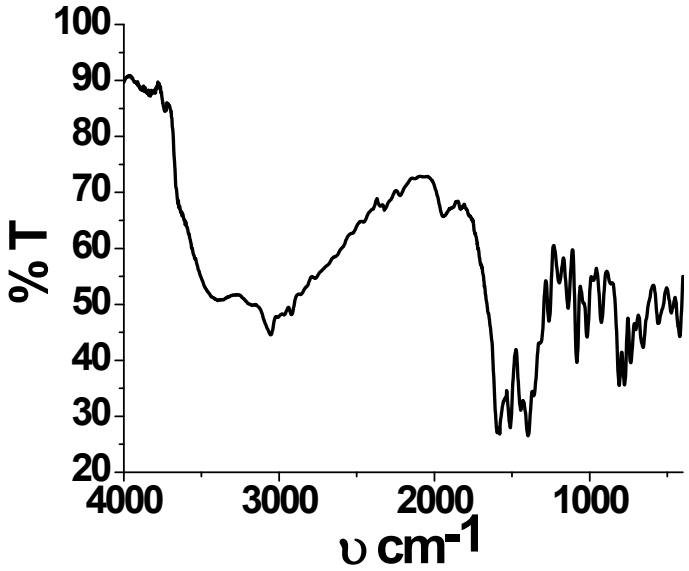

Fig. S13: IR spectrum of **2.**

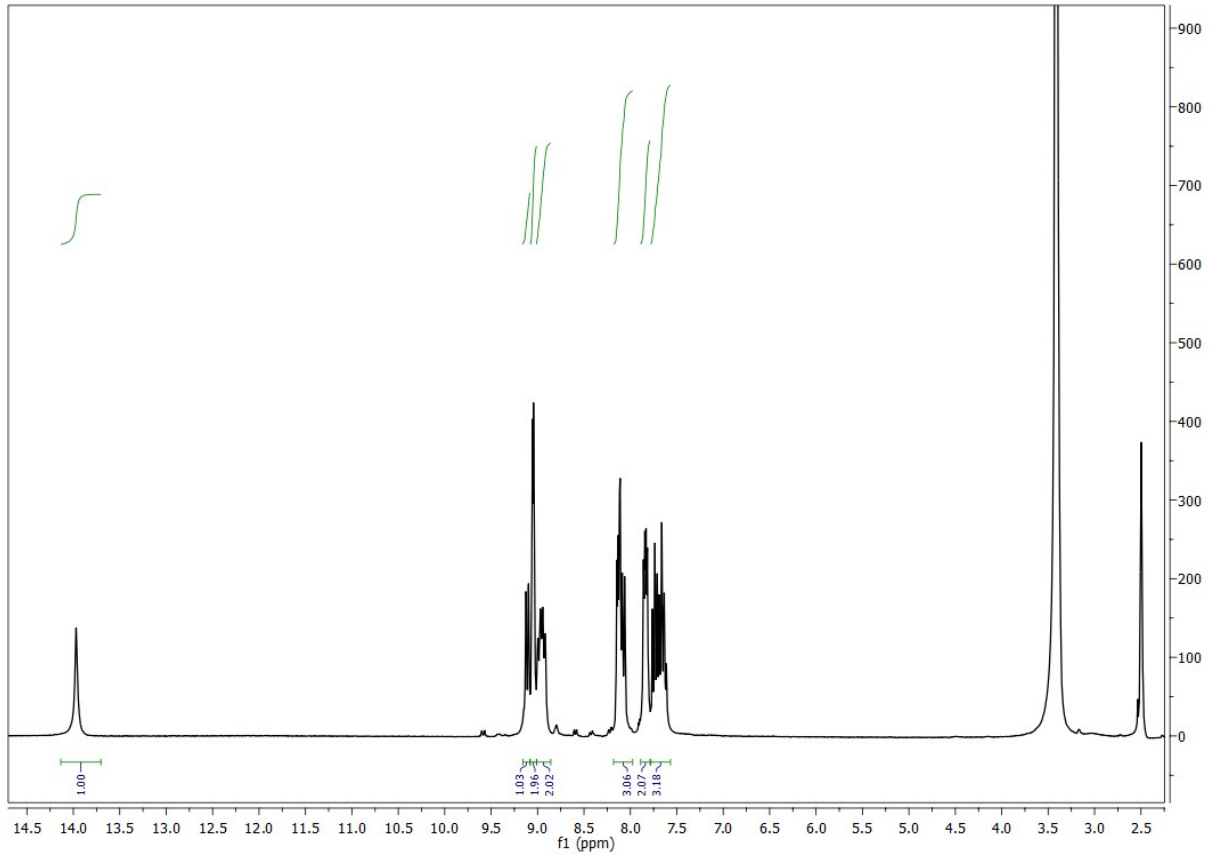

Fig. S14: ^{1}H-NMR spectrum of NIP recorded in DMSO-d^{6}

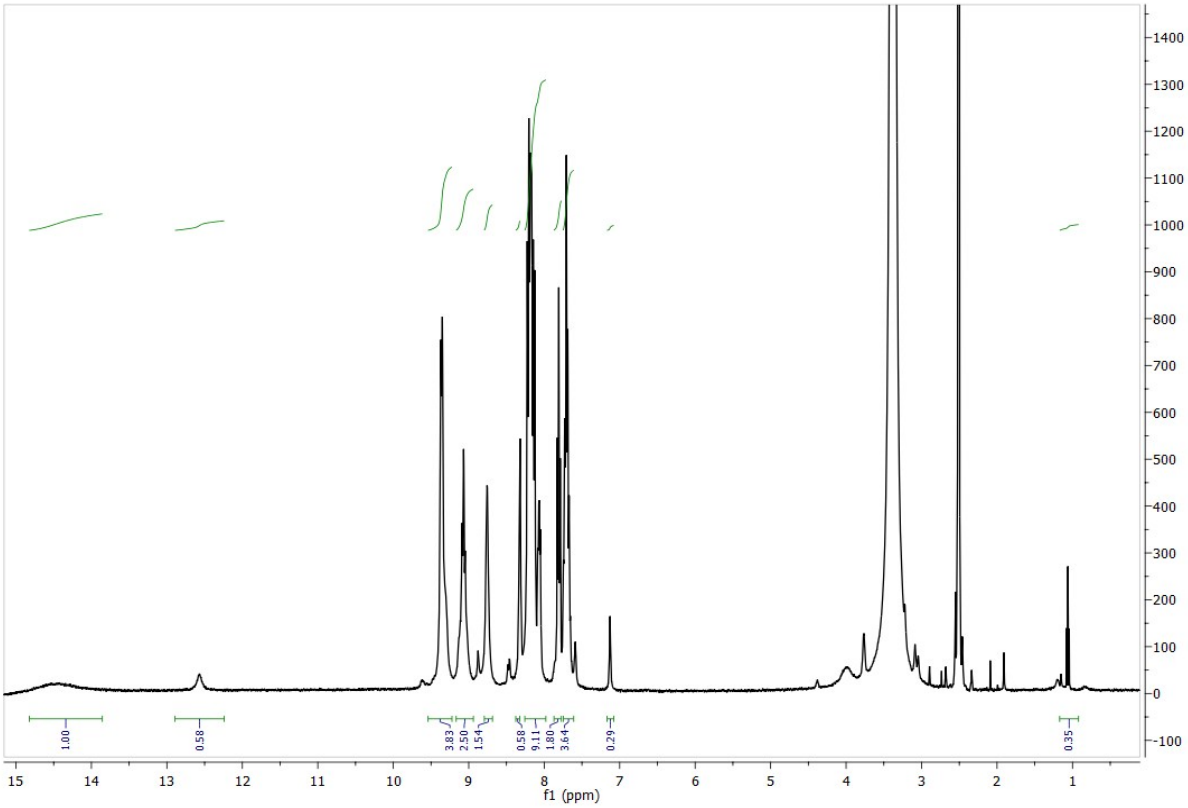

Fig. S15:[1]H-NMR spectrum of **1**recorded in DMSO-d6

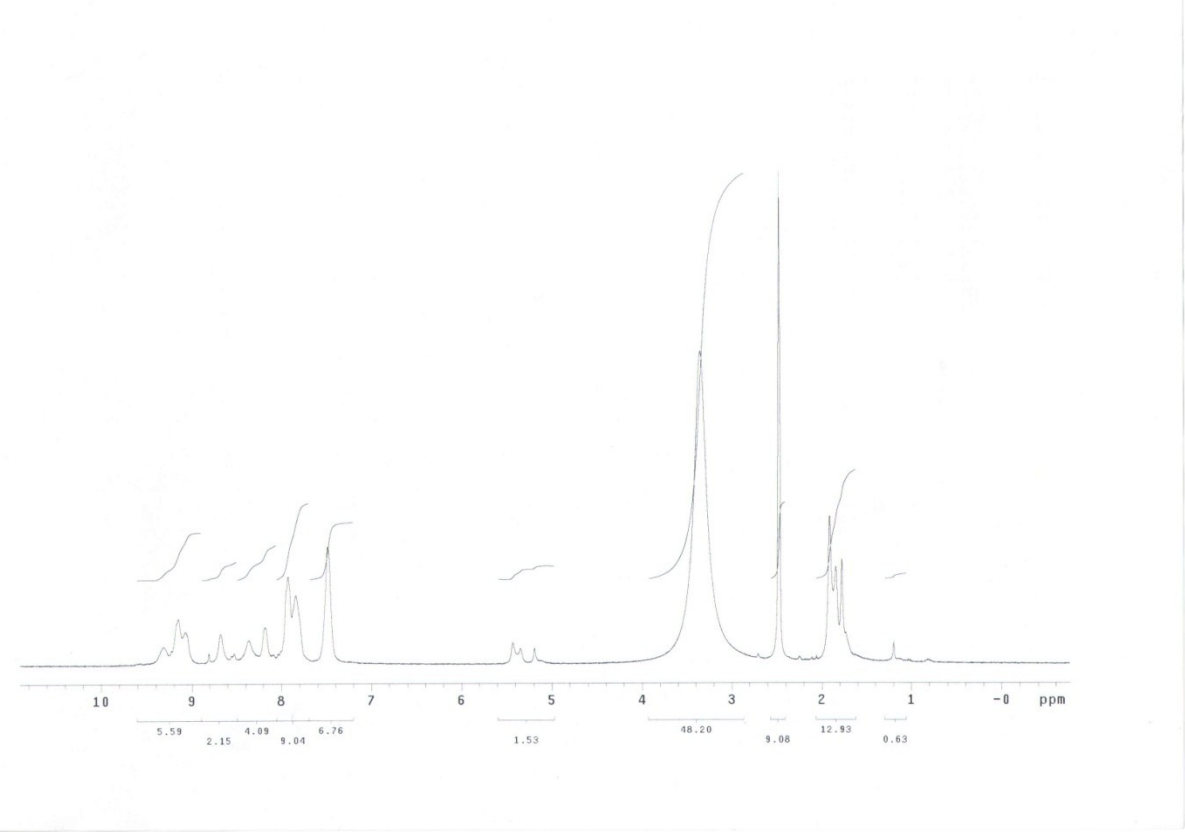

Fig. S16: ^{1}H-NMR spectrum of **2**recorded in DMSO-d6

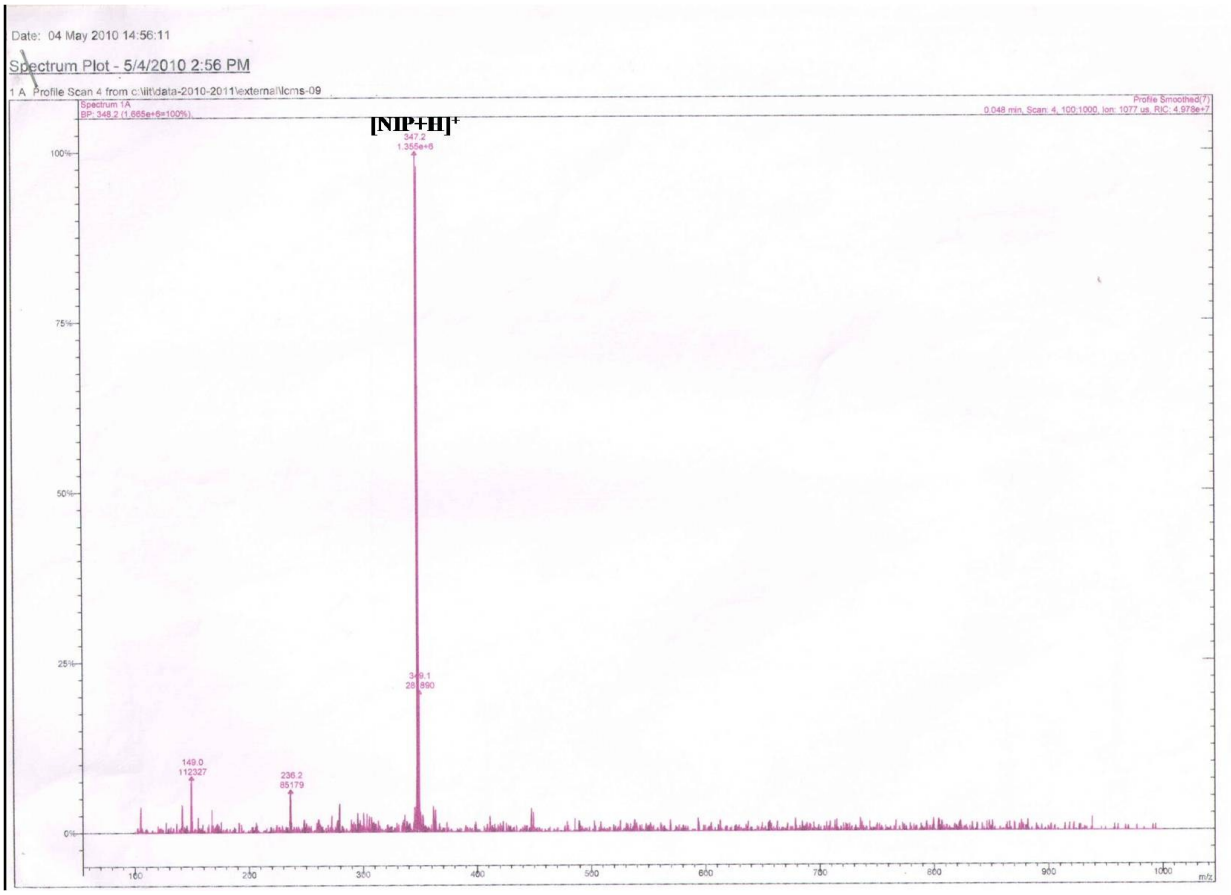

Fig. S17: ESI-MS spectrum of the ligand, NIP.

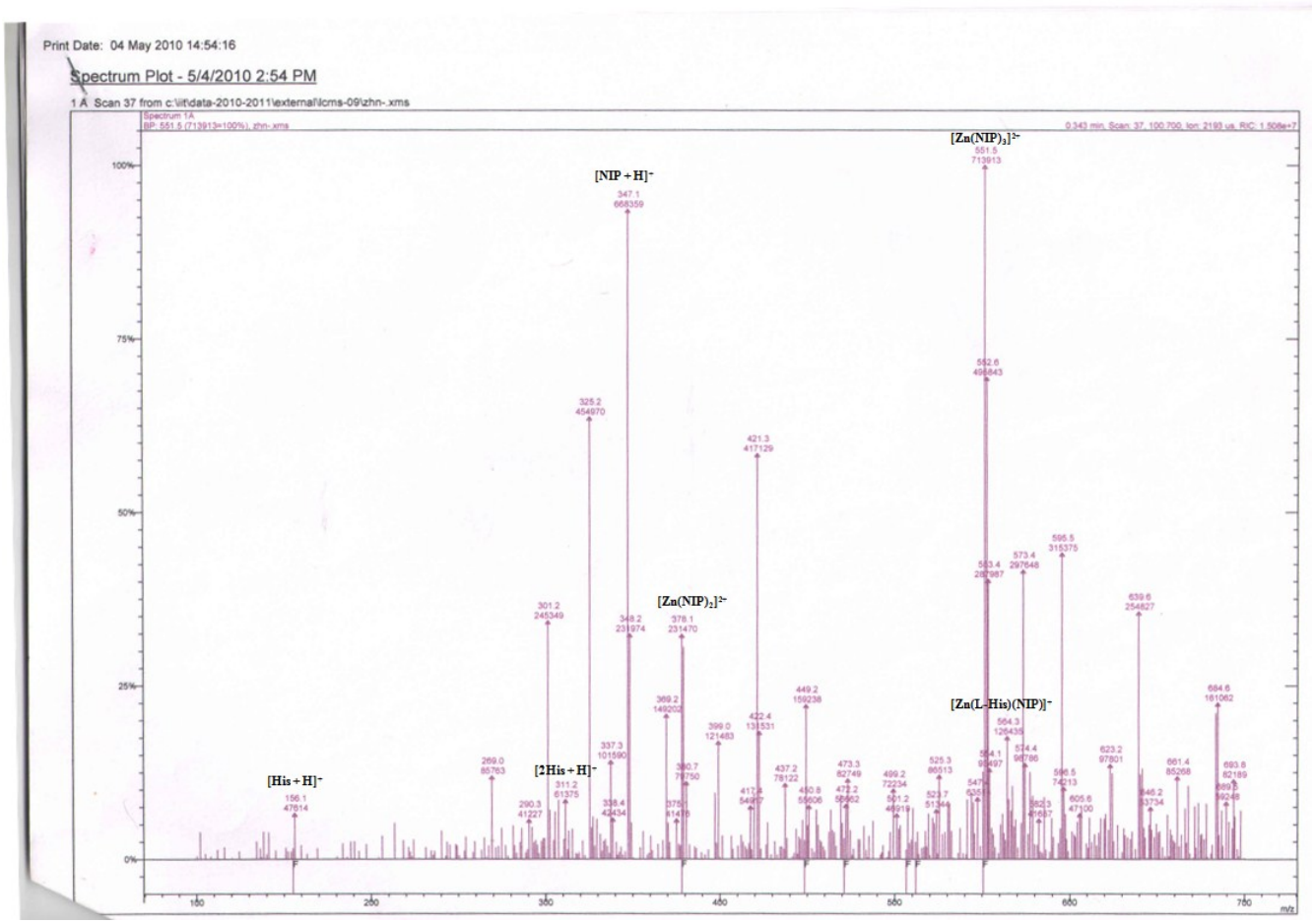

Fig. S18:ESI-MS spectrum of**1.**

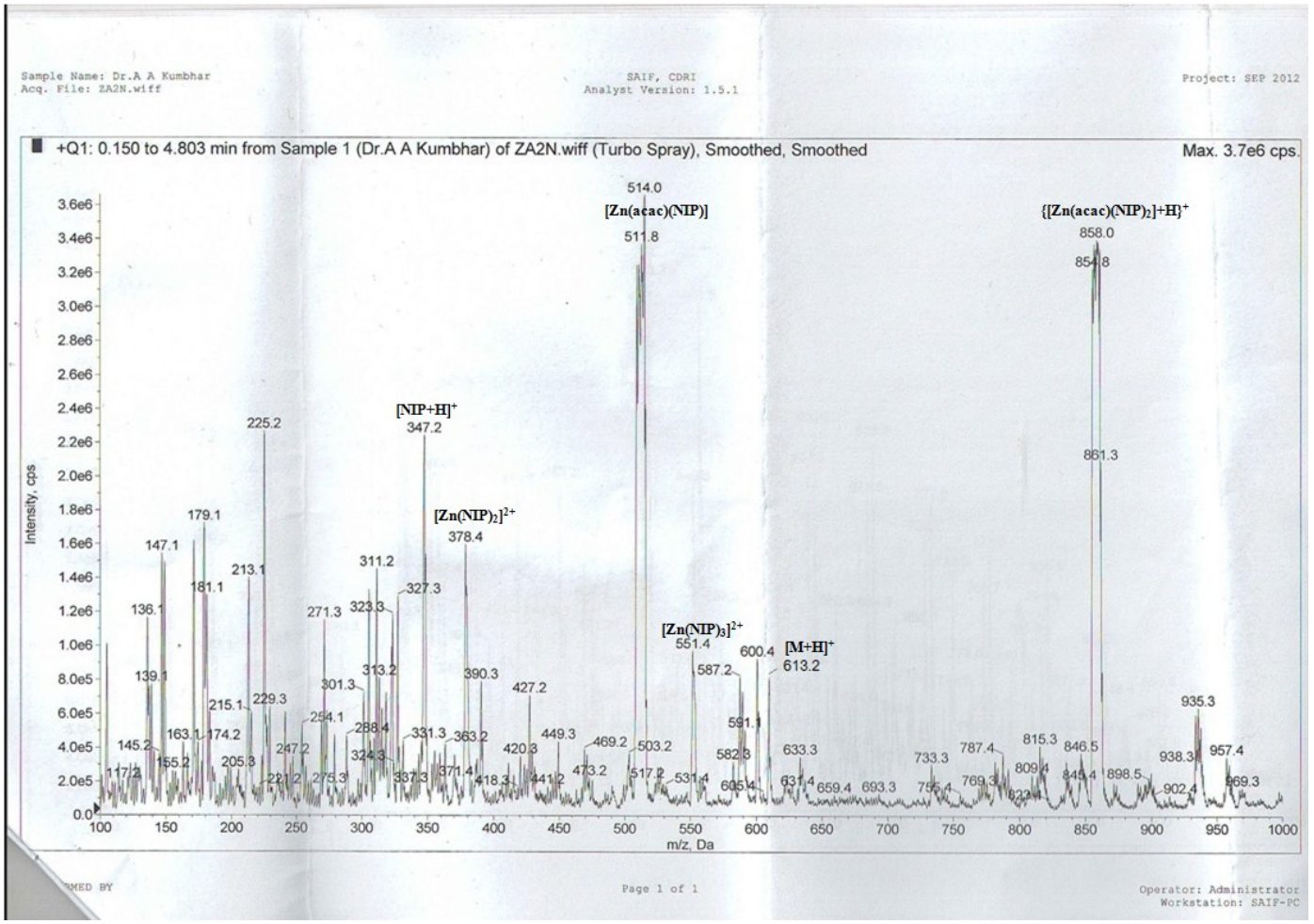

Fig. S19:ESI-MS spectrum of **2.**

References for Table S1.

1. S. S Bhat,A. A.Kumbhar,H.Heptullah,A. A.Khan,V. V.Gobre,S. P.Gejji, V. G.Puranik *Inorg. Chem*., **2011**, *50*, 545-558.

2. Q. L.Zhang,J. G.Liu,H.Chao, G. Q.Xue,L. N.Ji, *J. Inorg. Biochem*.,**2001**, *83*, 49-55.

3. P.Nagababu,M.Shilpa,J. N. L.Latha,I.Bhatnagar,P. N. B. S.Srinivas,Y. P. Kumar, K.L.Reddy,S.Satynarayana, *J. Fluoresc*., **2011**, *21*, 563-572.

4. Ji, L. N.;Zhang, Q. L.;Liu, J. G.;Liu, J. ; Xue, G. Q.;Li, H.;Liu,J. Z. *J. Inorg. Biochem*.,**2001**, *85*, 291-296.

5. L. N. Ji, Q. L. Zhang, J. G. Liu, J. Z. Liu, H. Li and Y. Yang, *Inorg. Chim. Acta*, 2002, **339**, 34-40.

6. L. N. Ji, L. F. Tan, H. Chao and Y. F. Zhou, *Polyhedron*, **2007**, *26*, 3029-3036.

7. L. N. Ji, L. F. Tan, H. Chao, H. Li and Y. J. Liu, *J. Inorg. Biochem*.,**2005**, *99*, 513-520.

8. C. C. Ju, A. G. Zhang, C. L. Yuan, X. L. Zhao, K. Z. Wang, *J. Inorg. Biochem*.,**2011**, ***105***, 435-443.

9.J. Tian, S. Yan, G. Chen, X. Qiao, P. Qiao, G. J. Xu, J. Y. Xu, W. Gu and X. Liu, *J. Inorg. Biochem*.,**2011**, *105*, 119–126.

10. S. Nagasubramanian, V. Thamilarasan, A. Jayamani, S. K. Kang, Y. Kim and N. Sengottuvelan, *Bull. Korean Chem. Soc*., **2013**, *34*, 1875-1878.